Full Facial Allotransplantation Including the Temporomandibular Joints: A Radiologic and Anatomical Cadaveric Study

Teresa Nunez-Villaveiran, M.D.
Vahe Fahradyan, M.D.
Edoardo Dalla Pozza, M.D.
Majid Rezaei, D.D.S., M.Sc.
Richard L. Drake, Ph.D.
Lyman M. Jellema, Ph.D.
Abelardo García-de-Lorenzo, M.D., Ph.D.
Frank A. Papay, M.D.
Bahar Bassiri Gharb, M.D., Ph.D.
Antonio Rampazzo, M.D., Ph.D.

Cleveland, Ohio; and Madrid, Spain

Background: Facial allotransplantation including the temporomandibular joints may improve the functional outcomes in face transplant candidates who have lost or damaged this joint.

Methods: Linear and angular measurements were taken in 100 dry skulls and mandibles and in 100 three-dimensionally–reconstructed facial computed tomographic scans to determine the variability of the temporomandibular joint, glenoid fossa, and mandible. A vascular study was performed in six fresh cadaveric heads, followed by harvest of the face allograft in three heads. Next, four heads were used for mock transplantation (two donors and two recipients). The full facial allograft included four different segments: a Le Fort III, a mandibular tooth-bearing, and two condyle and temporomandibular joint–bearing segments. Statistical analysis was performed using SAS software.

Results: In only one-third of the skulls, the condylar shape was symmetric between right and left sides. There was a wide variability in the condylar coronal (range, 14.3 to 23.62 mm) and sagittal dimensions (range, 5.64 to 10.96 mm), medial intercondylar distance (range, 66.55 to 89.91 mm), and intercondylar angles (range, 85.27 to 166.94 degrees). This high variability persisted after stratification by sex, ethnicity, and age. The temporomandibular joint was harvested based on the branches of the superficial temporal and maxillary arteries. The design of the allograft allowed fixation of the two condyle and temporomandibular joint–bearing segments to the recipient skull base, preserving the articular disk-condyle-fossa relationship, and differences were adjusted at the bilateral sagittal split osteotomy sites.

Conclusion: Procurement and transplantation of a temporomandibular joint–containing total face allograft is technically feasible in a cadaveric model. (*Plast. Reconstr. Surg.* 146: 621, 2020.)

Face allotransplantation shifted the paradigm of facial reconstruction more than a decade ago.[1,2] Since then, 46 facial transplantations have been performed worldwide, with a gradual increase in the complexity of the allograft and in the knowledge of the technique and the vascular anatomy.[3] In 2009, Cavadas et al. transplanted three-fourths of a mandible that included the

From the Department of Plastic Surgery, Cleveland Clinic; Cleveland Clinic Lerner College of Medicine of Case Western Reserve University; Physical Anthropology Laboratory, Cleveland Museum of Natural History; and the Department of Intensive Care, University Hospital "La Paz."

Received for publication July 14, 2019; accepted February 11, 2020.

Presented at the 75th Annual Meeting of the American Cleft Palate-Craniofacial Association, in Pittsburgh, Pennsylvania, April 10 through 14, 2018; the 7th Annual Meeting of the European Association of Plastic Surgeons Research Council, in Madrid, Spain, May 16 through 19, 2018; the 61st Annual Meeting of the Ohio Valley of Plastic Surgeons, in Cleveland, Ohio, June 1 through 2, 2018; Plastic Surgery The Meeting 2018, Annual Meeting of the American Society of Plastic Surgeons, in Chicago, Illinois, September 28 through October 1, 2018; the 6th Biennial Meeting of the American Society for Reconstructive Transplantation, in Chicago, Illinois, November 15 through 17, 2018; the 2019 Annual Meeting of the American Society for Reconstructive Microsurgery, in Palm Desert, California, February 2 through 5, 2019; the 53rd National Congress of the Spanish Society of Plastic, Reconstructive and Aesthetic Surgery, in Madrid, Spain, May 22 through 24, 2019; the 10th Congress of the World Society for Reconstructive Microsurgery, in Bologna, Italy, June 12 through 15, 2019; and the 18th Congress of the International Society of Craniofacial Surgery, in Paris, France, September 16 through 19, 2019.

DOI: 10.1097/PRS.0000000000007069

left condyle.[4] This is the only reported case that included part of the temporomandibular joint in the facial allograft. To date, there are no reported cases of a full face transplant including mandible and the temporomandibular joints. Although inclusion of the temporomandibular joints within a facial allograft has the potential to improve the outcomes in a selected group of patients with damaged or ankylosed joints, high variability of condylar shape, intercondylar distance, and intercondylar angle in the population makes the transfer of temporomandibular joints between donors and recipients difficult.[5–13] Moreover, proximity to important anatomical structures such as the internal carotid artery and the brain, which could be damaged during the harvest, with potential consequences for the procurement of the other organs, adds further complexity to the procedure. The goal of this study was to design a transplant model that included a Le Fort III, mandible, and both temporomandibular joints in a cadaveric model that could be easily adopted in patients with different anatomy.

MATERIALS AND METHODS

Evaluation of the Variability of Mandible and Temporomandibular Joint Dimensions

Measurements in Dry Skulls and Mandibles

We selected a sample of 100 dry skulls of the Hamann-Todd Collection (Cleveland Museum of Natural History, Cleveland, Ohio). The sample included 50 African American and 50 European American skulls (each group with 25 female and 25 male skulls) with an age range between 21 and 65 years. Measurements were taken with a digital protractor (GemRed "Quick 360" Digital Angle Rule, Guangxi, People's Republic of China) and caliper (Mitutoyo Digimatic, Mitutoyo Corp., Kanagawa, Japan). The shape of the condyles,[14] the dimensions of the condyles, ramus, intercondylar distances,[15] gonial angle, intercondylar angle, and condyle-symphysis angle[16] were recorded. (**See Figure, Supplemental Digital Content 1**, which shows the shape of the condyle, which was evaluated in the horizontal, frontal, and sagittal planes (*above, center*, and *below*, respectively). The shape of the condyle was described, from left to right, as cylindric, elliptical, or irregular for the horizontal plane; as flat, gabled, or slightly rounded for the frontal plane; and as convex (whole contour arched outward), locally concave (some part of the contour arched inward), or wedged (flat anterior and posterior surfaces that converged together in a wedge shape) in the sagittal plane, ***http://links.lww.com/PRS/E156***. **See Figure, Supplemental Digital Content 2**, which shows anatomical landmarks of the mandible: posterior mandibular condyle (*PCo*), anterior mandibular condyle (*ACo*), lateral mandibular condyle (*LCo*), medial mandibular condyle (*MCo*), superior mandible condyle (*SCo*), inferior sigmoid notch (*InfSig*), pogonion (*Pog*), posterior superior mandibular condyle (*PSCo*), and gonion (*Go*), ***http://links.lww.com/PRS/E157***. **See Figure, Supplemental Digital Content 3**, which shows linear measurements of the mandible: condylar length, condylar width, condylar height, and lateral mandibular condyle to gonion (*above, right*, and *above, left*, respectively). Maximum mandibular width, lateral mandibular condyle to gonion, maximum lateral intercondylar distance, and maximum medial intercondylar distance (*below, right*, and *below, left*, respectively) are also shown, ***http://links.lww.com/PRS/E158***. **See Figure, Supplemental Digital Content 4**, which shows angular measurements of the mandible and condyle: the intercondylar angle (*ICA*) is measured as the angle formed by the intersection of the lines drawn through the long axis of each condyle. The condyle-symphysis angle (*CSA*) is measured as the angle formed by the intersection of lines drawn from the center of the condylar neck to the midline of the anterior border of the symphysis. The gonial angle is the angle formed by a line drawn tangent to the lower border of the mandible and a line touching the posterior border of the ramus at two points, one at the condyle and one at the gonion, ***http://links.lww.com/PRS/E159***.] Dimensions of the glenoid fossae and the distances between the right and left fossae were measured.[13]

Measurements in Three-Dimensionally–Reconstructed Facial Computed Tomographic Scans

With approval of the institutional review board, 100 facial computed tomographic scans were selected to include 21- to 65-year-old patients

Disclosure: *There are no sources of support that require acknowledgment. The authors have no financial or personal relationships with other people or organizations that could influence (bias) this work inappropriately. The authors have no financial interest in any of the products or devices mentioned in this work.*

Related digital media are available in the full-text version of the article on www.PRSJournal.com.

with no history of mandibular disease or trauma. Three-dimensional images of the computed tomographic scans were obtained. Measurements were performed using ImageJ software (50i; National Institutes of Health, Bethesda, Md.). Three reference planes (axial, coronal, and midsagittal) were established for orientation. Angular measurements performed included the intercondylar angle, gonial angle, frontal ramal angle, lateral ramal angle, and the angle between the condylar and glenoid fossa axis (condylar angle) with the intermastoid line.[16,17] [**See Figure, Supplemental Digital Content 5**, which shows angles measured in three-dimensionally–reconstructed facial computed tomographic scans: frontal ramal angle (*above, left*), lateral ramal angle (*above, right*), condylar and intercondylar angle (*below, left*), and gonial angle (*below, right*). *Po*, porion; *Or*, orbitale; *Cdlat*, condylion lateralis; *Cdpost*, condylion posterius; *Gopost*, gonion posterius; *Golat*, gonion lateralis; *ICA*, intercondylar angle; *CA*, condylar angle; *GA*, gonial angle; *FRA*, frontal ramal angle; *LRA*, lateral ramal angle, ***http://links.lww.com/PRS/E160***.]

Anatomical Study in Fresh Cadavers

In eight fresh heads, both common carotid arteries were injected with red latex (Carolina Biological, Burlington, N.C.) and dissected. In 10 hemifaces, the external carotid artery and its branches were dissected. In three heads, a full-face allograft, including a Le Fort III, a mandibular tooth-bearing segment, and two condyle and temporomandibular joint–bearing segments, was harvested (Fig. 1). Short bilateral sagittal split osteotomies[18] were performed. Laterally, the temporalis muscle was excised to expose the temporalis bone. The external auditory canal was divided to expose the mastoid bone. A temporal bone craniotomy was performed. The temporal lobe dura was elevated along the floor of the middle cranial fossa. The internal carotid artery was then identified anteriorly at the level of the foramen lacerum. The bone above the horizontal portion of the internal carotid artery was removed until the genu was exposed (Fig. 2). The posterior osteotomy was then performed down to the carotid foramen (Fig. 3), to expose the vertical segment of the artery, through the petrous portion of the temporal bone, and the middle of the bony ear canal to include the postglenoid process in the flap (Fig. 4). The anterior osteotomy was performed anterior to the temporomandibular joint, through the zygomatic arch and through the squamous portion of the temporal bone anterior to the origin of the zygomatic process up to the foramen ovale, with preservation of the foramen spinosum and middle meningeal artery (Fig. 2) for vascularization of the temporal bone. The medial osteotomy was next completed, between the foramen ovale and the exposed internal carotid artery (Fig. 2). Capsular attachments of the temporomandibular joint and the temporomandibular ligament were preserved. At this point the flap, including the Le Fort III, the mandibular tooth-bearing segment, and the two condyle and temporomandibular joint–bearing segments, was

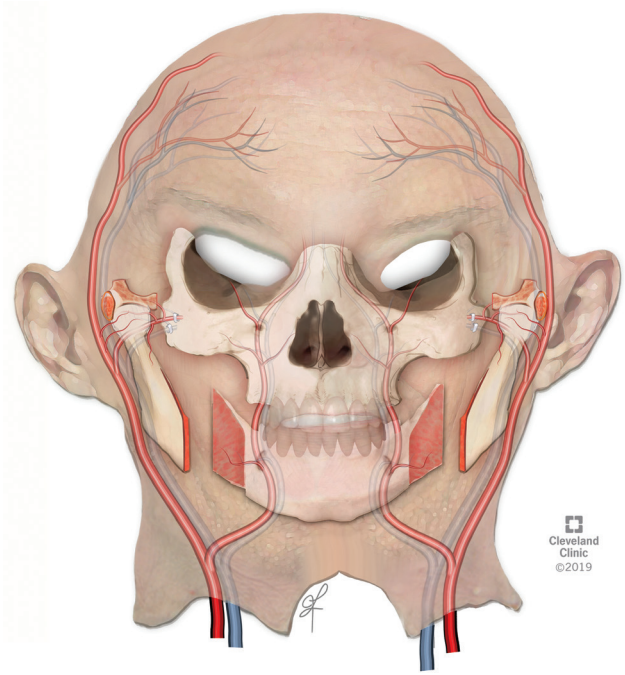

Fig. 1. Facial allotransplantation illustration. A facial allograft is shown containing a Le Fort III, a mandibular tooth-bearing segment, and two smaller condyle and temporomandibular joint–bearing segments. The mandibular tooth-bearing segment and the Le Fort III segment are vascularized by the branches of the facial artery. In particular, the mental arteries enter the mandibular tooth-bearing segment through the mental foramen, and the infraorbital artery enters the Le Fort III segment through the infraorbital foramen. The superficial temporal and maxillary arteries supply the two smaller condyle and temporomandibular joint–bearing segments. The external carotid arteries and internal jugular veins are used as the donor vessels where the anastomosis would be performed. This design, based on different vessels, allows the fixation of the two smaller condyle and temporomandibular joint–bearing segments on the recipient skull base first, followed by the Le Fort III and tooth-bearing segments increasing flexibility of the inset. (Reprinted with permission, Cleveland Clinic Center for Medical Art & Photography © 2019. All rights reserved.)

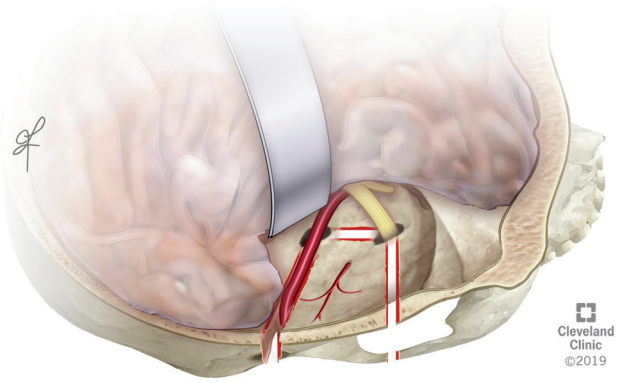

Fig. 2. Cranial view of the skull base osteotomies. The course of the internal carotid artery is the most important landmark during the harvest of the temporomandibular joint. The internal carotid artery is identified anteriorly, and it is exposed from anterior to posterior until the genu is identified. The vertical osteotomy goes through the middle of the external auditory meatus up to the carotid canal. The anterior osteotomy ends at the level of the foramen ovale. The medial osteotomy connects the osteotomy at the foramen lacerum to the foramen ovale. The middle meningeal artery, taking off from the maxillary artery and entering the skull base through the foramen spinosum, is preserved for vascularization of the temporal bone. (Reprinted with permission, Cleveland Clinic Center for Medical Art & Photography © 2019. All rights reserved.)

completely raised on the branches of the external carotid artery (Fig. 5).

In one cadaver, resin EpoxAcast 690 (Smooth-On, East Texas, Pa.) was injected into the common carotid artery. The same osteotomies to harvest the condyle and temporomandibular joint–bearing segments were performed and the sample was

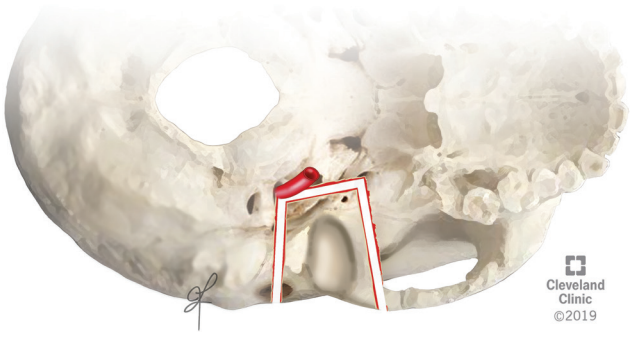

Fig. 3. Caudal view of the skull base osteotomies. The posterior osteotomy, going through the middle of the external auditory meatus, exposes the lateral surface of the internal carotid artery from the external opening up to the genu of the carotid canal. The foramen spinosum is included in the flap. (Reprinted with permission, Cleveland Clinic Center for Medical Art & Photography © 2019. All rights reserved.)

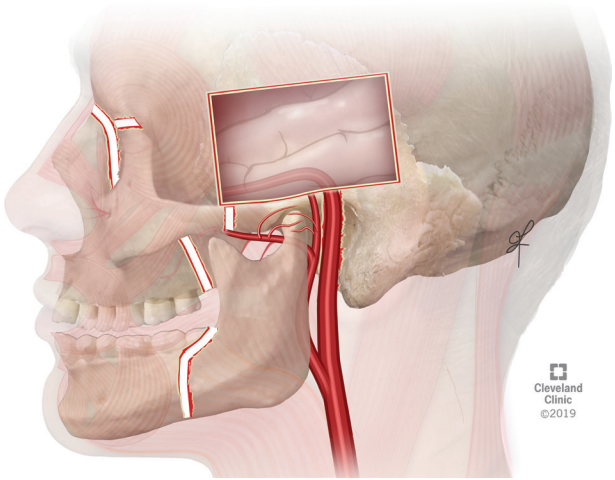

Fig. 4. Lateral view of the temporal bone and mandibular osteotomies. The internal carotid artery is exposed through the posterior osteotomy. The postglenoid process is included in the flap. The anterior skull base osteotomy is placed through the zygomatic process of the temporal bone. The condyle and temporomandibular joint–bearing segment is vascularized by branches of the superficial temporal and maxillary arteries. The Le Fort III and bilateral sagittal split osteotomies are also shown. (Reprinted with permission, Cleveland Clinic Center for Medical Art & Photography © 2019. All rights reserved.)

submerged for 72 hours in pure bleach to remove the soft tissues.

Mock Transplantation

Four cadavers were used to simulate a full face and temporomandibular joint transplantation. Harvest of the full-face allograft including

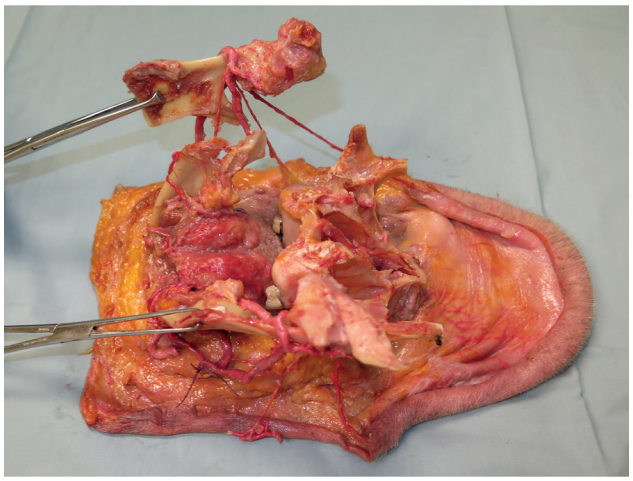

Fig. 5. Posterolateral view of a full facial cadaveric allograft. A Le Fort III segment, a mandibular tooth-bearing segment, and the two condyle and temporomandibular joint–bearing segments are completely harvested based on the branches of the external carotid artery.

temporomandibular joints from the donor was performed as described earlier. A recipient defect was created by removing the Le Fort III segment and the mandible. The cartilage of the glenoid fossa of the recipient was completely removed. Next, the donor allograft was transferred to the recipient face. The donor temporomandibular joint was fixed to the recipient glenoid fossa, ensuring maximum bony contact between the temporal bone of the donor and recipient. Rigid fixation was achieved between the donor temporal bone and the zygomatic arch of the recipient's face with two bicortical screws. The Le Fort III osteotomy sites were fixed at the nasion and lateral orbital rims. Next, the maxillomandibular fixation was performed with maximal dental intercuspation. Bony defects between the proximal and distal mandibular segments were bone grafted, to preserve the donor frontal ramal angle in the coronal plane, intercondylar angle in the axial plane, and lateral ramal angle and centric relation of the joint in the sagittal plane. If bigonial width of the donor mandible was excessive compared to the recipient, the distal bone of the tooth-bearing segment was shaved. Plates and unicortical screws were used at the bilateral sagittal split osteotomy sites. Donor mandibular rami were shortened if long. The maxillomandibular fixation was released and the final occlusion and unrestricted range of motion of the mandible was confirmed. Computed tomographic images of the donor and recipient heads were taken before and after the transplantation. Three-dimensional cephalometric analysis was performed with Dolphin 11.95 (Dolphin Imaging & Management Solutions, Chatsworth, Calif.).

Statistical Analysis

Statistical analyses were completed using SAS 9.3 (SAS Institute, Inc., Cary, N.C.). Tests were two-tailed and values of $p < 0.05$ were considered statistically significant. The McNemar test was used to compare the right and left condylar shape. The Pearson correlation coefficient was used to investigate the relationship between age and quantitative data. The independent samples *t* test was used to assess differences between sexes, ethnicities, and age (older than 40 or younger than 40 years). A general linear model (or a multivariant model of repeated measures analysis of variance for measurements was performed on both sides), with a post hoc Bonferroni correction, were used to test the combined effect of sex, ethnicity, age, and side on the observed measurements.

RESULTS

Evaluation of the Variability of Mandible and Temporomandibular Joint Dimensions

Condyle Shape

The most common configuration was cylindrical, slightly rounded, and locally concave. [**See Table, Supplemental Digital Content 6**, which shows condylar shape percentages for the right and left condylar shapes. Condylar shapes are described for the horizontal, frontal, and sagittal planes (Solberg WK, Hansson TL, Nordström B. The temporomandibular joint in young adults at autopsy: A morphologic classification and evaluation. *J Oral Rehabil.* 1985;12:303–321. 10.1111/j.1365-2842.1985.tb01285.x). The first letter corresponds to the shape in the horizontal plane (*E*, elliptical; *C*, cylindrical; *I*, irregular), the second letter corresponds to the shape in the frontal plane (*R*, rounded; *F*, flat; *G*, gabled), and the last letter corresponds to the shape in the sagittal plane (*C*, convex; *L*, locally concave; *W*, wedged), ***http://links.lww.com/PRS/E161***.] Only 33 percent of the patients had symmetrical right and left condylar shapes in the three planes. There was a significant difference in the shape of the right and left condyles in the horizontal plane ($p = 0.016$) (Tables 1 through 3). T1-T3

Mandible and Skull Base Dimensions

The mean condylar coronal and sagittal dimensions were 19.42 mm (range, 14.3 to 23.62 mm)

Table 1. Shapes of the Right and Left Condyle in the Horizontal Plane

	Left*			
	Cylindrical	Elliptical	Irregular	Total
Right				
Cylindrical	40	4	5	49
Elliptical	16	22	0	38
Irregular	4	3	6	13
Total	60	29	11	100

*McNemar-Bowker $p = 0.016$; $\kappa = 0.450$.

Table 2. Shapes of the Right and Left Condyle in the Frontal Plane

	Left*			
	Flat	Gabled	Slightly Rounded	Total
Right				
Flat	24	3	7	34
Gabled	1	1	3	5
Slightly rounded	10	5	46	61
Total	35	9	56	100

*McNemar-Bowker $p = 0.566$; $\kappa = 0.458$.

Table 3. Shapes of the Right and Left Condyle in the Sagittal Plane

	Left*			
	Convex	Locally Concave	Wedge	Total
Right				
Convex	18	12	3	33
Locally concave	13	27	5	45
Wedge	4	10	8	22
Total	35	49	16	100

*McNemar-Bowker $p = 0.604$; $\kappa = 0.253$.

and 8.28 mm (range, 5.64 to 10.96 mm), respectively. The mean glenoid fossa coronal and sagittal dimensions were 24.85 ± 1.69 mm and 15.46 ± 1.17 mm, respectively. The mean medial intercondylar distance was 78.47 mm (range, 66.55 to 89.91 mm). There was a wide variability in the bigonial distance, mandibular sagittal length, and mandibular ramus height (Table 4). Age and sex both had a significant effect on the transverse dimension of the condyle and medial intercondylar distance (Table 5).

Three-Dimensional Facial Computed Tomographic Scans

The mean frontal ramal angle was 78.18 degrees (range, 70.28 to 88.25 degrees) (Table 6). There was a significant difference between the right and left sides ($p = 0.015$) and male and female sexes ($p = 0.003$). Significant differences between ethnicities were found for all the parameters except for frontal ramal angle (Table 7). The axes of the condyle and glenoid fossa were always parallel. The condylar angle and intercondylar angle were very variable: mean, 21.98 degrees (range, 5.83 to 48.64 degrees) and 135.64 degrees (range, 85.27 to 166.94 degrees), respectively (Fig. 6 and Table 6).

Linear Measurements and Angles

A high variability in the different linear measurements and angles was present even after stratification by sex, ethnicity, and age. Increased age (41 to 65 years versus 21 to 40 years) significantly correlated with an increased intercondylar distance (MCo–MCo and LCo–LCo) in all subgroups except in the male Caucasian subgroup (Table 8).

Table 4. Descriptive Statistics for All Parameters Measured in Dry Skulls and Mandibles*

	Value (mm)
MCo–LCo	
Average ± SD	19.42 ± 1.90
Range	14.3–23.62
FTR	
Average ± SD	24.85 ± 1.69
Range	20.69–31.27
PCo–ACo	
Average ± SD	8.28 ± 1.15
Range	5.64–10.96
FAP	
Average ± SD	15.46 ± 1.17
Range	10.97–19.99
CoHt	
Average ± SD	20.15 ± 2.87
Range	13.42–28.73
ICA	
Average ± SD	140.42 ± 10.09
Range	118.9–162.5
LCo–LCo	
Average ± SD	115.17 ± 6.48
Range	98.02–128.00
LFD	
Average ± SD	116.69 ± 5.86
Range	101.65–129.08
MCo–MCo	
Average ± SD	78.47 ± 4.88
Range	66.55–89.91
MFD	
Average ± SD	71.36 ± 4.40
Range	60.52–82.76
Go–Go	
Average ± SD	95.13 ± 6.80
Range	82.70–115.33
CSA	
Average ± SD	64.46±5.61
Range	53.4–77.1
Pog–PSCo	
Average ± SD	124.75 ± 6.55
Range	108.01–137.48
LCo–Go	
Average ± SD	55.25±7.93
Range	37.35–72.16
GA	
Average ± SD	124.37 ± 7.09
Range	107.45–147.45

MCo–LCo, condylar width; FTR, transverse fossa dimension; PCo–ACo, condylar length; FAP, anteroposterior fossa dimension; CoHt, condylar height; ICA, intercondylar angle; LCo–LCo, maximum lateral intercondylar distance; LFD, lateral fossa–to–lateral fossa distance; MCo–MCo, maximum medial intercondylar distance; MFD, medial fossa–to–medial fossa distance; Go–Go, maximum mandibular width; CSA, condyle-symphysis angle; Pog–PSCo, pogonion to condyle; LCo–Go, lateral mandibular condyle to gonion; GA, gonial angle.
*Values are in millimeters.

Anatomical Study in Fresh Cadavers

The temporomandibular joint capsule was richly vascularized in all specimens. Posteriorly and laterally, most of the branches came directly from the superficial temporal artery and/or the transverse facial artery (Fig. 7). Medially and anteriorly, branches were given by the maxillary artery directly, and/or by the middle meningeal, the masseteric, the deep temporal, and the tympanic arteries (Fig. 8). The temporal bone was always vascularized by the middle meningeal artery (Fig. 9). The diameter of the terminal branches ranged between 0.3 to 0.4 and 0.7 to 0.8 mm.

Table 5. Summary of Effects of Side, Sex, Ethnicity, and Age in Measurements Performed in Dry Skulls and Mandibles

	Measurement Difference (95% CI)			Age Effect	Post Hoc Analysis: Interactions and Effects ($p < 0.05$)
	Side	Sex	Ethnicity		
MCo-LCo, mm	NS	1.74 (1.09–2.39)	0.74 (0.00–1.48) ($p = 0.051$)	$R = 0.19$ ($p = 0.06$)	Interaction side plus sex plus ethnicity Effect of age, sex, and ethnicity
FTR, mm	NS	1.15 (0.50–1.80)	0.93 (0.26–1.61)	NS	Interaction age and side Effect of sex and ethnicity
PCo-ACo, mm	NS	0.44 (0.04–0.84) ($p = 0.057$)	0.85 (0.45–1.25)	NS	No interactions Effect of sex and ethnicity
FAP	NS	NS	NS	NS	No interactions No effects
CoHt, mm	NS	2.04 (0.94–3.14)	NS	NS	Interaction side and sex and ethnicity Effect of sex
ICA, deg	NA	NS	5.25 (1.36–9.13)	NS	No interactions Effect ethnicity
LCo–LCo, mm	NA	5.87 (3.57–8.17)	NS	$R = 0.393$ ($p < 0.001$)	Interaction sex plus ethnicity Effect age and sex
LFD, mm	NA	6.79 (4.88–8.70)	NS	NS	No interactions Effect of sex
MCo–MCo, mm	NA	2.13 (0.23–4.03)	NS	$R = 0.404$ ($p < 0.001$)	No interactions Effect age and sex
MFD, mm	NA	3.27 (1.64–4.90)	NS	$R = 0.216$ ($p = 0.031$)	Interaction sex and ethnicity Effect age and sex
GO–GO, mm	NA	7.72 (5.48–9.96)	2.91 (0.24–5.57)	NS	No interactions Effect sex and ethnicity
CSA, deg	NA	NS	3.04 (0.88–5.19)	NS	No interactions Effect ethnicity
Pog–PSCo, mm	0.63 (0.13–1.13)	8.74 (6.90–10.63)	NS	NS	No interactions Effect of sex
LCo – Go, mm	NS	7.74 (10.38–5.11)	3.59 (0.48–6.71)	NS	No interactions Effect of sex and ethnicity
GA, deg	0 .97 (0.28–1.67)	3.91 (1.23–6.58)	3.03 (−0.02 to 6.09)	NS	Interaction side and ethnicity, and side and gender and ethnicity Effect of age and ethnicity

LCo–LCo, maximum lateral intercondylar distance; NS, not significant; FTR, transverse fossa dimension; PCo–ACo, condylar length; FAP, anteroposterior fossa dimension; CoHt, condylar height; ICA, intercondylar angle; NA, not applicable; LCo–LCo, maximum lateral intercondylar distance; LFD, lateral fossa–to–lateral fossa distance; MCo–MCo, maximum medial intercondylar distance; MFD, medial fossa–to–medial fossa distance; Go–Go, maximum mandibular width; CSA, condyle-symphysis angle; Pog–PSCo, pogonion to condyle; LCo–Go, lateral mandibular condyle to gonion; GA, gonial angle.

*Differences between the right and left sides (paired *t* test), and the effects of age [Pearson correlation coefficient (*R*)], sex, and ethnicity (independent samples *t* test) on measurements in dry skulls and mandibles. Post hoc analyses were performed using multivariant model of repeated measures analysis of variance for parameters measured on both sides, and a general linear model was performed for the rest of parameters to determine whether there were interactions between side, sex, ethnicity, and age. Post hoc comparisons were performed with the Bonferroni correction applied to the means estimated by the studied model. Only significant differences or values of *p* close to significance are shown.

The harvest of the allograft took 4 hours. The Le Fort III and the mandibular tooth-bearing segments were vascularized by branches of the facial arteries, and the two condyle and temporomandibular joint–bearing segments were vascularized by branches of the superficial temporal and maxillary arteries, pedicled on the bilateral external carotid arteries. The internal carotid artery was never damaged.

Mock Transplantation

Both transplants took 7.5 hours. The intercondylar distance (LCo–LCo) increased in both transplants (12.7 and 5.2 mm), as did the bigonial distance (1.6 mm and 9.4 mm) compared to the recipient. The intercondylar angle decreased 21.5 degrees in the first transplant and increased 6 degrees in the second transplant compared to the donor. The frontal ramal angle decreased in both transplants compared to the donor (5.6 and 7 degrees, respectively), as did the lateral ramal angle (37.5 and 3.5 degrees, respectively). In the first transplant, 8-mm shortening of the pogonion-to-condyle distance and counterclockwise rotation of the occlusal plane resulted in a 4.7-degree decrease in sella-nasion–A point angle and a 9.8-degree increase in sella-nasion–B point angle compared to the recipient. In the second transplant, 5.3-mm shortening of the

Table 6. Descriptive Statistics for All Parameters Measured on the Three-Dimensional Computed Tomographic Scans

	Value (deg)
FRA	
Average ± SD	78.18 ± 3.67
Range	70.28–88.25
LRA	
Average ± SD	82.17 ± 5.46
Range	70.44–96.66
GA	
Average ± SD	122.47 ± 7.21
Range	107.51–136.98
CA	
Average ± SD	21.98 ± 8.02
Range	5.83–48.64
ICA	
Average ± SD	135.64 ± 15.34
Range	85.27–166.94

FTR, transverse fossa dimension; LRA, lateral ramal angle; GA, gonial angle; CA, condylar angle; ICA, intercondylar angle.

pogonion-to-condyle distance and clockwise rotation of the occlusal plane caused a 12.3-degree and an 11.5-degree decrease in sella-nasion–A point angle and sella-nasion–B point angle compared to the recipient (Table 9). Facial angles in the first and second transplants were 180 and 182 degrees, respectively. The range of motion for mouth opening was 40 mm and smooth in the first cadaver. The second cadaver achieved Angle class 1 occlusion and the lateral excursion was 10 mm, protrusion was 5 mm, and interincisal distance was 45 mm (Fig. 10). [**See Video (online)**, which shows an animation of the three-dimensionally–reconstructed facial computed tomographic scan after the second mock transplantation. Frontal, oblique, lateral, and caudal views show the range of motion of the mandible. The donor temporomandibular joint is secured on top of the recipient glenoid fossa. Two bicortical screws are used for fixation of the donor temporal bone to the recipient zygomatic arch to avoid any violation of the temporomandibular joint.]

DISCUSSION

A normal temporomandibular joint is typified by the following functional characteristics: the ability of articulating surfaces to move painlessly within a required range of motion, proper load distribution, stability during function, and support for the dentition in an interdigitated occlusal position.[19] The structure of the temporomandibular joint appears to be very sensitive to any functional loading. Any factor that changes the biomechanics of the temporomandibular joint or masticatory system can provoke its remodeling and change its structure.[20–22] For these reasons, alterations in the condylar position from surgery can lead to malocclusion associated with the risk of early relapse[23] and the development of temporomandibular disorders.[24–26]

Therefore, proper harvest and fixation of the two donor condyle and temporomandibular joint–bearing segments with the Le Fort III and the mandibular tooth-bearing segment become key steps during facial transplantation. Based on their extensive experience with orthognathic surgery, Epker and Wylie insisted that the maintenance of the normal presurgical anatomical position of the mandibular condyles and contiguous proximal

Table 7. Summary of the Effect of Side, Sex, Ethnicity, and Age on Facial Three-Dimensional Computed Tomographic Scan Measurements

	Mean Measurement Difference (95% CI)				
	Side	Sex	Ethnicity	Age Effect	Post Hoc Analysis: Interactions and
FRA, mm	0.76 (0.15–1.36)	2.18 (0.79–3.58)	NS	NS	No interactions Effect of sex, side
LRA, deg	NS	NS	4.32 (2.28–3.37)	$R = -0.215$ ($p = 0.032$)	No interactions Effect of ethnicity
GA, deg	NS	NS	3.91 (1.07–6.73)	NS	No interactions Effect ethnicity
CA, deg	NS	NS	5.38 (2.31–8.44)	$R = 0.202$ ($p = 0.043$)	No interactions Effect of ethnicity
ICA	NS	NS	10.67 (4.83–16.50)	NS	No interactions Effect of ethnicity

FRA, frontal ramal angle; LRA, lateral ramal angle; GA, gonial angle; CA, condylar angle; ICA, intracondylar angle; NS, not significant.
*This table summarizes the differences between the right and left sides (paired *t* test), and the effects of age [Pearson correlation coefficient (*R*)], sex, and ethnicity (independent samples *t* test) on measurements performed on facial three-dimensional computed tomographic scans. Post hoc analyses were performed using multivariant model of repeated measures analysis of variance for parameters measured on both sides, and a general linear model was performed for the rest of parameters to determine whether there was interaction between side, sex, ethnicity, and age. Post hoc comparisons were performed with the Bonferroni correction applied to the means estimated by the studied model. Only significant differences or values of *p* close to significance are shown.

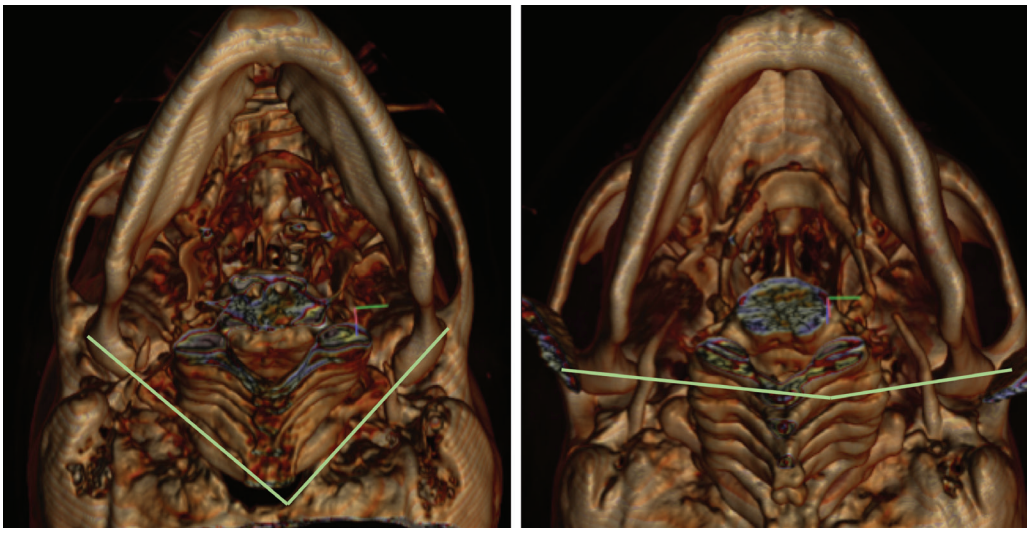

Fig. 6. Caudal views of three-dimensionally–reconstructed facial computed tomographic scans. These two individuals show a major difference in their intercondylar angles and axes of the glenoid fossas. This is one of the reasons why a hybrid joint between a recipient skull base and donor condylar head will not work. This mismatch would cause condylar sagging, reabsorption, relapse, temporomandibular joint arthritis, and malocclusion.

Table 8. Age Effect in African American Women, Caucasian Women, African American Men, and Caucasian Men

	Average ± SD (Range)			
	21–40 Yr	41–65 Yr	*R* (Pearson)	*p* (*t* test)
African American women				
MCo–LCo, mm	18.44 ± 1.67 (15.39–21.04)	19.41 ± 1.85 (16.17–22.9)	0.230	0.207
PCo–ACo, mm	8.65 ± 0.70 (7.55–9.86)	8.47 ± 1.17 (5.72–10.44)	–0.136	0.681
ICA, deg	134.86 ± 6.77 (125–149.3)	137.55 ± 8.07 (125.7–148.1)	0.021	0.406
LCo–LCo, mm	111.12 ± 6.36 (99.84–117.96)	115.36 ± 5.59 (103.52–123.29)	0.410† ($p = 0.04$)	0.097
MCo–MCo, mm	76.32 ± 4.33 (68.66–81.47)	78.36 ± 3.54 (73.11–84.77)	0.407† ($p = 0.04$)	0.214
FRA (CT scan), deg	77.64 ± 3.81 (71.22–82.48)	75.46 ± 2.51 (70.42–78.68)	–0.339	0.104
LRA (CT scan), deg	83.18 ± 6.97 (73.29–96.34)	84.56 ± 5.87 (77.88–95.36)	0.111	0.593
Caucasian women				
MCo–LCo, mm	17.56 ± 1.82 (14.3–19.82)	18.41 ± 1.58 (16.79–21.15)	0.220	0.223
PCo–ACo, mm	7.56 ± 1.46 (5.79–10.22)	7.60 ± 1.02 (5.64–9.28)	0.006	0.927
ICA, deg	140.95 ± 10.98 (120.4–157.7)	144.43 ± 11.51 (119.3–160.3)	0.163	0.451
LCo–LCo, mm	107.38 ± 6.24 (98.02–117.39)	113.19 ± 5.90 (103.93–123.3)	0.464† ($p = 0.02$)	0.026†
MCo–MCo, mm	74.72 ± 5.18 (66.55–82.31)	79.11 ± 4.95 (71.97–88.13)	0.471† ($p = 0.02$)	0.042†
FRA (CT scan), deg	78.21 ± 2.74 (75.23–82.29)	77.21 ± 3.17 (73.25–85.65)	–0.141	0.453
LRA (CT scan), deg	81.92 ± 5.69 (73.88–90.86)	79.44 ± 3.07 (73.72–86.26)	–0.298	0.201
African American men				
MCo–LCo, mm	19.93 ± 1.42 (17.43–21.4)	20.90 ± 1.77 (17.97–23.62)	0.381	0.159
PCo–ACo, mm	8.48 ± 1.34 (7.01–10.96)	9.14 ± 0.74 (7.83–10.67)	0.330	0.125
ICA, deg	137.14 ± 8.55 (120.7–150.1)	140.26 ± 7.54 (128–151.4)	0.117	0.347
LCo–LCo, mm	113.83 ± 5.72 (104.61–120.57)	120.02 ± 3.52 (114.19–124.11)	0.633† ($p < 0.001$)	0.003†
MCo–MCo, mm	76.05 ± 4.68 (67.07–81.51)	80.49 ± 4.52 (71.97–88.02)	0.442† ($p = 0.03$)	0.026†
FRA (CT scan), deg	79.86 ± 3.76 (72.38–88.25)	78.82 ± 3.05 (72.27–82.26)	–0.114	0.485
LRA (CT scan), deg	84.77 ± 5.55 (75.46–96.66)	84.50 ± 2.52 (81.76–90.29)	–0.256	0.893
Caucasian men				
MCo – LCo (mm)	20.08 ±1.64 (17.69–22.5)	20.04 ±1.38 (16.83–22.58)	0.026	0.939
PCo – ACo (mm)	8.24 ± 1.01 (6.76–10.13)	8.04 ± 0.99 (6.73–10.7)	–0.107	0.638
ICA (°)	140.28 ± 15.03 (118.9–160.1)	145.13 ± 9.38 (130.7–162.5)	0.261	0.329
LCo-LCo (mm)	117.40 ± 4.53 (111.77–123.46)	119.50 ± 4.64 (109.65–128)	0.306	0.275
MCo – MCo (mm)	78.74 ± 3.76 (71.25–82.94)	81.43 ± 5.14 (73.7–89.91)	0.360	0.170
FRA (CT scan), deg	79.73 ± 4.09 (70.28–83.72)	78.73 ± 4.19 (72.99–87.50)	–0.185	0.555
LRA (CT scan), deg	80.69 ± 4.50 (71.52–89.00)	78.08 ± 4.76 (70.44–87.94)	–0.432† ($p = 0.03$)	0.173

MCo–LCo, condylar width; PCo–ACo, condylar length; ICA, intercondylar angle; LCo–LCo, maximum lateral intercondylar distance; MCo–MCo, maximum medial intercondylar distance; FRA, frontal ramal angle; LRA, lateral ramal angle.
*Comparison of measurements (Pearson correlation coefficient and *t* test) in the different subpopulations according to the different ages (aged 21–40 yr vs. 41–65 yr).
†Statistically significant.

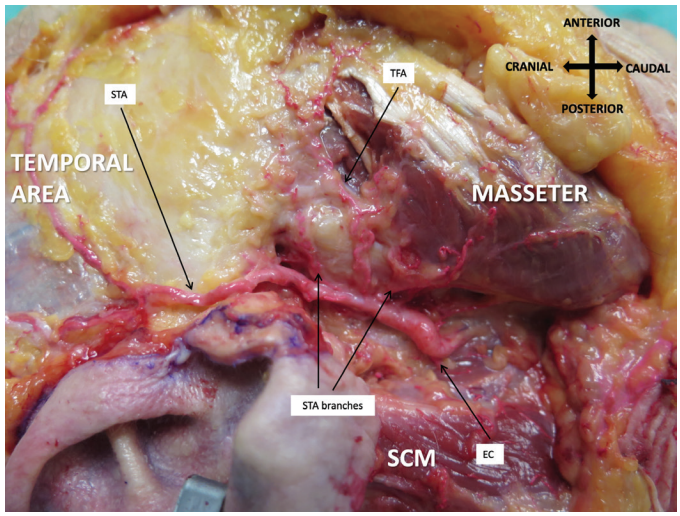

Fig. 7. Posterolateral vascularization of the condyle. This cadaver was injected in the external carotid artery with red colored latex. The condyle is vascularized posterior and laterally by branches that come directly from the superficial temporal artery (*STA*) and the transverse facial artery (*TFA*). *EC*, external carotid artery, *SCM*, sternocleidomastoid muscle.

mandibular ramal segment was very important to ensure the stability of the surgical result, to reduce the adverse effects on the temporomandibular joint, and to improve the masticatory function.[27] For the above reasons, we designed a full facial allograft including four different segments: a Le Fort III, a mandibular tooth-bearing segment, and two condyle and temporomandibular joint–bearing segments. This design allowed the fixation of the two condyles and temporomandibular joint–bearing segments first, with preservation of the donor articular disk-condyle-fossa relationship. This was achieved during the fixation of the donor temporomandibular joint onto

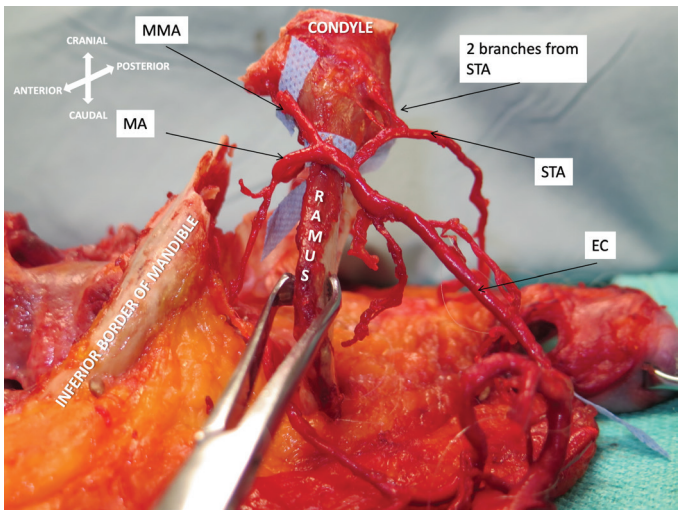

Fig. 8. Vascularization of the temporomandibular joint. Posterior view from the mandibular angle to the temporomandibular joint (including the temporal bone) in a cadaver injected with red colored latex. Two branches arising from the superficial temporal artery (*STA*) and one branch from the middle meningeal artery (*MMA*) supply the temporomandibular joint. There were also three branches arising directly from the maxillary artery (*MA*) in this specimen that are not seen from this projection. *EC*, external carotid artery.

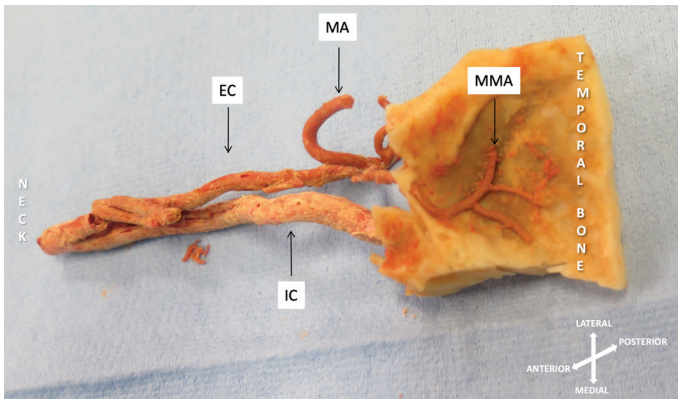

Fig. 9. Vascularization of the skull base. This specimen was injected with resin in the common carotid artery and was then submerged for 72 hours in pure bleach. The middle meningeal artery (*MMA*) is shown entering the skull base through the foramen spinosum and suppling the temporal bone with its branches. *EC*, external carotid artery; *IC*, internal carotid artery; *MA*, maxillary artery.

the recipient skull base with preservation of the donor condylar angle in the axial plane, frontal ramal angle in the coronal plane and lateral ramal angle, and centric relation in the sagittal plane overall preventing medial or lateral inclination of the ramus, axial torquing, and condylar sagging of the temporomandibular joint. A similar concept is used during temporomandibular joint total joint replacement where the fossa component of the prosthesis is inserted on top of the recipient glenoid fossa and stabilized to the zygomatic arch.[28,29] Once the Le Fort III segment was plated and the maxillomandibular fixation was applied, any bony discrepancy between the tooth-bearing and the condylar-bearing fragments was addressed with either bone grafts or by shaving the bone interferences, to avoid any tridimensional change of the temporomandibular joint. Considering that 30 mm was the difference between the minimal and maximal intercondylar distance in our study, an adjustment of at most 15 mm at each bilateral sagittal split osteotomy site was sufficient to match any donor and recipient. This technique prevents modification of the condylar position and can be used independently from the anatomy of the donor and recipient.[8,12,13,30–32] Furthermore, this

Table 9. Measurements in Donors, Recipients, and Hybrid Faces after Mock Transplantation

	Parameters in Donors, Recipients, and Transplant Simulations					
	Donor 1	Recipient 1	Transplant 1	Donor 2	Recipient 2	Transplant 2
LCo–LCo, mm	120.2	117.9	130.6	120.1	115.3	120.5
LFD, mm	125.2	120.4	125.6	120.6	118.9	147.7
MCo–MCo, mm	93.4	83.4	106.9	83.3	82.1	81.5
MFD, mm	82.9	75.5	79.6	77.6	71.6	79.3
Go–Go, mm	89.5	89.9	91.5	95.5	93.1	102.5
CSA, deg	77.2	71.9	77.6	71.6	61.4	72.9
Pg–PSCo, mm	110.2	121.3	113.3	117.7	112.1	106.8
LCo–Go, mm	53	51.4	52.6	53.1	52.3	43.9
ICA, deg	122.5	142	101	147	123	153
CA, deg	28.75	19	39.5	16.5	28.5	13.5
FRA, deg	76.1	76.9	70.5	79.9	77.4	72.9
LRA, deg	98	93	60.5	86.5	77.5	83.0
GA, deg	120.7	123.1	122.9	124.4	131.8	121.9
SNA, deg	87.1	90.8	86.1	89.7	85.9	73.6
SNB, deg	82.1	83.2	93.0	82.7	84.6	73.1
Facial angle (G′-Sn′-Pg′)	165	160.5	180	171	163	182

LCo–LCo, maximum lateral intercondylar distance; LFD, lateral fossa–to–lateral fossa distance; MCo–MCo, maximum medial intercondylar distance; MFD, medial fossa–to–medial fossa distance; Go–Go, maximum mandibular width; CSA, condyle-symphysis angle; Pog-PSCo, pogonion to condyle; LCo–Go, lateral mandibular condyle to gonion; ICA, intercondylar angle; CA, condylar angle; GA, gonial angle; FRA, frontal ramal angle; LRA, lateral ramal angle; GA, gonial angle; SNA, sella-nasion–A point angle; SNB, sella-nasion–B point angle; Facial angle (G′-Sn′-Pg′), soft-tissue glabella-subnasale-pogonion angle.

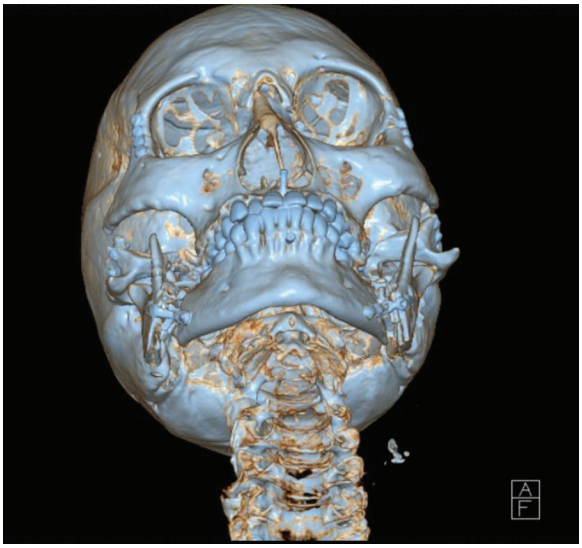

Fig. 10. Three-dimensionally–reconstructed computed tomographic scan of the second mock transplantation. The temporomandibular joint is secured onto the recipient skull base. The condylar angle was preserved and the condyle is in centric relation. Bone grafts were used between the tooth-bearing fragment and two condyle and temporomandibular joint–bearing segments to avoid modification of the frontal ramal angle.

technique can be used for unicondylar or bicondylar face transplantation in the setting of temporomandibular joint destruction and ankylosis.[33]

Yale et al. described 32 different composite mandibular condyle types in 2950 samples studied.[8] In a study by Solberg et al.,[14] 39 percent of the temporomandibular joints displayed mild to marked deviation in form in all three components of the joint and disk displacement in 12 percent. A high variability of the intercondylar distance and angle has been also reported.[13,30–32] In this study, 24 different condylar head configurations were found, and after stratification of the condylar and mandibular measurements by age, sex, ethnicity, and side, there was still a high variability between the subpopulations.

Transplantation of the intact donor mandible with bilateral condyles to the recipient skull base by creating a hybrid temporomandibular joint as described by Khavanin et al.[34,35] has several limitations considering the high anatomical variability found in our study even after stratification by sex, age, and race. Differences in the condyle shape, size, intercondylar distance, angle, violation of the capsule, and lubricant mechanism would cause a high risk for ankylosis of the joint. Resuspension of the condyle with a suture from the glenoid fossa would reduce the movement from a gliding and hinging joint to a pure hinging joint around the insertion of the suture. Furthermore, reduction of the donor condyle into a recipient skull base with different intercondylar distances and angles, based on the "condylar window" as suggested, would create localized compressive and/or tensile forces that will predominate in different areas of the condyle.[36] Peripheral condylar sagging would occur with the condyle positioned inferiorly with peripheral contact with the fossa while the teeth are in occlusion. Delayed occlusal relapse would occur as a result of condylar resorption or change in its shape.[37] As the condyles progressively reabsorb, the mandible would progressively retrude, affecting adversely both the mechanical function of the joint and the occlusion.[19,21] Cavadas et al.[4] reported only 10-mm mandible excursion at 16 months postoperatively after mandible and unilateral condylar transplantation, which confirms the above limitations. In another study by Khavanin et al.,[35] procurement of an allograft as a contiguous unit, including the mandible, temporal bone, and midface maintaining the zygomatic arch, was described. Again, a difference in the intercondylar distance and the gnathic index[13] between the donor and recipient would increase the inset difficulty. Details on inclusion of the temporal bone were also not reported.

The intracranial approach to the temporomandibular joint, described here, includes a wide temporal craniectomy to have a better exposure of the joint from above to visualize and preserve the route of the internal carotid artery. Complete exposure of the internal carotid artery to access critical cranial base structures through the petrosal bone is well described in the neurosurgery literature, and we used a similar technique.[38,39]

Vascularization of the temporomandibular joint was found to be rich and provided by branches of the middle meningeal artery, superficial temporal, transverse facial, maxillary, masseteric branch, and/or deep temporal arteries. These findings are in agreement with recent publications describing an arterial quadrangle formed by the superficial temporal (posterior), the posterior deep temporal and the masseteric arteries (anterior), and the maxillary (medial) and the transverse facial arteries (lateral) around the condyle.[40–44] We previously reported that after the injection of contrast in the homolateral facial artery, contrast was present in only 66.7 percent of the condyles.[45] The two condyle and temporomandibular joint–bearing segments were therefore harvested based on the terminal branches of the external carotid artery (superficial temporal and maxillary artery up to the middle meningeal artery) to improve vascularization and freedom during inset. The Le Fort III and mandibular tooth-bearing segments were

pedicled on the facial arteries, which has been reported clinically to be reliable.[45–48]

The transplantation procedure proved to be feasible based on this design, with good range of motion of the mandible. An increase in the intercondylar distance and the bigonial angle is to be expected after the operation. The bilateral sagittal split and Le Fort III osteotomies allowed us to modify the occlusal plane as routinely performed during orthognathic procedures.[49]

CONCLUSIONS

This study was performed in a cadaveric model and focused mainly on the bony and vascular aspects of the temporomandibular joint transplantation. Inherent limitations of this study are reliability of the vascularization findings because of the possible variability of the injection technique and inability of a cadaver model to truly assess temporomandibular joint dynamics and occlusion in addition to long-term adverse outcomes such as ankylosis and trismus. Future studies regarding the dynamics of mastication following face transplantation including the temporomandibular joints are warranted. Temporomandibular joint–containing total face allograft procurement and transplantation was technically feasible in this cadaveric model.

Antonio Rampazzo, M.D., Ph.D.
Department of Plastic Surgery
Cleveland Clinic
9500 Euclid Avenue
Cleveland, Ohio 44195
rampaza@ccf.org
Instagram: @antonio.rampazzo
Facebook: antonio.rampazzo.md

ACKNOWLEDGMENTS

The authors would like to thank Rosario Madero, Ph.D. (Biostatistics Unit, University Hospital "La Paz", Madrid, Spain), for invaluable help with the statistical analysis; Jeff Loerch for creating the illustrations; Susan Lopez, Ryan Klatte, and Mark Sabo for editing the videos; and Carli Siegel, C.N.P., for proofreading the article.

REFERENCES

1. Devauchelle B, Badet L, Lengelé B, et al. First human face allograft: Early report. *Lancet* 2006;368:203–209.
2. Siemionow M, Papay F, Alam D, et al. Near-total human face transplantation for a severely disfigured patient in the USA. *Lancet* 2009;374:203–209.
3. Siemionow M. The decade of face transplant outcomes. *J Mater Sci Mater Med.* 2017;28:64.
4. Cavadas PC, Ibáñez J, Thione A. Surgical aspects of a lower face, mandible, and tongue allotransplantation. *J Reconstr Microsurg.* 2012;28:43–47.
5. Pandis N, Karpac J, Trevino R, Williams B. A radiographic study of condyle position at various depths of cut in dry skulls with axially corrected lateral tomograms. *Am J Orthod Dentofacial Orthop.* 1991;100:116–122.
6. Dumas AL, Oaddab MB, Homayoun NH, McDonough J. A three-dimensional developmental measurement of the temporomandibular joint. *Cranio* 1986;4:22–35.
7. Yale SH, Rosenburg HM, Ceballos M, Haupt-Fuehrer JD. Laminagraphic cephalometry in the analysis of mandibular condyle morphology: A preliminary report. *Oral Surg Oral Med Oral Pathol.* 1961;14:793–805.
8. Yale SH, Allison BD, Hauptfuehrer JD. An epidemiological assessment of mandibular condyle morphology. *Oral Surg Oral Med Oral Pathol.* 1966;21:169–177.
9. Taylor RC, Ware WH, Fowler D, Kobayashi J. A study of temporomandibular joint morphology and its relationship to the dentition. *Oral Surg Oral Med Oral Pathol.* 1972;33:1002–1013.
10. Moses AJ, Bonato RA, Pacini GL. Consideration of intercondylar angles in determining a maxillo-mandibular relationship for intraoral sleep appliances. *EG Sleep Diagn Ther.* 2012;7:41–49.
11. Parr NM, Passalacqua NV, Skorpinski K. Investigations into age-related changes in the human mandible. *J Forensic Sci.* 2017;62:1586–1591.
12. Martin DC, Danforth ME. An analysis of secular change in the human mandible over the last century. *Am J Hum Biol.* 2009;21:704–706.
13. Wish-Baratz S, Hershkovitz I, Arensburg B, Latimer B, Jellema LM. Size and location of the human temporomandibular joint. *Am J Phys Anthropol.* 1996;101:387–400.
14. Solberg WK, Hansson TL, Nordström B. The temporomandibular joint in young adults at autopsy: A morphologic classification and evaluation. *J Oral Rehabil.* 1985;12:303–321.
15. Hilgers ML, Scarfe WC, Scheetz JP, Farman AG. Accuracy of linear temporomandibular joint measurements with cone beam computed tomography and digital cephalometric radiography. *Am J Orthod Dentofacial Orthop.* 2005;128:803–811.
16. Hackney FL, Van Sickels JE, Nummikoski PV. Condylar displacement and temporomandibular joint dysfunction following bilateral sagittal split osteotomy and rigid fixation. *J Oral Maxillofac Surg.* 1989;47:223–227.
17. Kim KS, Son WS, Park SB, Kim SS, Kim YI. Relationship between chin deviation and the position and morphology of the mandible in individuals with a unilateral cleft lip and palate. *Korean J Orthod.* 2013;43:168–177.
18. Hunsuck EE. A modified intraoral sagittal splitting technic for correction of mandibular prognathism. *J Oral Surg.* 1968;26:250–253.
19. Arnett GW, Milam SB, Gottesman L. Progressive mandibular retrusion: Idiopathic condylar resorption. Part I. *Am J Orthod Dentofacial Orthop.* 1996;110:8–15.
20. Arnett GW, Milam SB, Gottesman L. Progressive mandibular retrusion: Idiopathic condylar resorption. Part II. *Am J Orthod Dentofacial Orthop.* 1996;110:117–127.
21. Arnett G, Gunson M. Risk factors in the initiation of condylar resorption. *Semin Orthod.* 2013;19:81–88.
22. Lin H, Zhu P, Lin Y, et al. Mandibular asymmetry: A three-dimensional quantification of bilateral condyles. *Head Face Med.* 2013;9:42.
23. Harada K, Okada Y, Nagura H, Enomoto S. A new condylar positioning appliance for two-jaw osteotomies (Le Fort I and sagittal split ramus osteotomy). *Plast Reconstr Surg.* 1996;98:363–365.
24. Isberg AM, Isacsson G. Tissue reactions of the temporomandibular joint following retrusive guidance of the mandible. *Cranio* 1986;4:143–148.

25. Ellis E III, Hinton RJ. Histologic examination of the temporomandibular joint after mandibular advancement with and without rigid fixation: An experimental investigation in adult *Macaca mulatta*. *J Oral Maxillofac Surg*. 1991;49:1316–1327.
26. Rotskoff KS, Herbosa EG, Villa P. Maintenance of condyle-proximal segment position in orthognathic surgery. *J Oral Maxillofac Surg*. 1991;49:2–7; discussion 7–8.
27. Epker BN, Wylie GA. Control of the condylar-proximal mandibular segments after sagittal split osteotomies to advance the mandible. *Oral Surg Oral Med Oral Pathol*. 1986;62:613–617.
28. Wolford LM, Pitta MC, Reiche-Fischel O, Franco PF. TMJ Concepts/Techmedica custom-made TMJ total joint prosthesis: 5-year follow-up study. *Int J Oral Maxillofac Surg*. 2003;32:268–274.
29. Pearce CS, Cooper C, Speculand B. One stage management of ankylosis of the temporomandibular joint with a custom-made total joint replacement system. *Br J Oral Maxillofac Surg*. 2009;47:530–534.
30. Giles E. Sex determination by discriminant function analysis of the mandible. *Am J Phys Anthropol*. 1964;22:129–135.
31. Lazić B, Tepavcević B, Keros J, Komar D, Stanicić T, Azinović Z. Intercondylar distances of the human temporomandibular joints. *Coll Antropol*. 2006;30:37–41.
32. Eisenburger M, Haubitz B, Schmelzeisen R, Wolter S, Tschernitschek H. The human mandibular intercondylar angle measured by computed tomography. *Arch Oral Biol*. 1999;44:947–951.
33. Krezdorn N, Alhefzi M, Perry B, et al. Trismus in face transplantation following ballistic trauma. *J Craniofac Surg*. 2018;29:843–847.
34. Khavanin N, Davidson EH, Lee DY, Byrne P, Dorafshar AH. Anatomic considerations for temporomandibular joint vascularized composite allotransplantation. *J Craniofac Surg*. 2018;29:871–877.
35. Khavanin N, Davidson EH, Smith RM, Macmillan A, Byrne P, Dorafshar AH. Considerations for temporomandibular joint procurement in vascularized composite allotransplantation. *J Craniofac Surg*. 2018;29:1742–1746.
36. Moore KE, Gooris PJ, Stoelinga PJ. The contributing role of condylar resorption to skeletal relapse following mandibular advancement surgery: Report of five cases. *J Oral Maxillofac Surg*. 1991;49:448–460.
37. Reyneke JP, Ferretti C. Intraoperative diagnosis of condylar sag after bilateral sagittal split ramus osteotomy. *Br J Oral Maxillofac Surg*. 2002;40:285–292.
38. Vilela MD, Rostomily RC. Temporomandibular joint-preserving preauricular subtemporal-infratemporal fossa approach: Surgical technique and clinical application. *Neurosurgery* 2004;55:143–153; discussion 153–154.
39. Kutz JW Jr, Mitchell D, Isaacson B, et al. En bloc resection of the temporal bone and temporomandibular joint for advanced temporal bone carcinoma. *Otolaryngol Head Neck Surg*. 2015;152:571–573.
40. Touré G, Duboucher C, Vacher C. Anatomical modifications of the temporomandibular joint during ageing. *Surg Radiol Anat*. 2005;27:51–55.
41. Saka B, Wree A, Anders L, Gundlach KK. Experimental and comparative study of the blood supply to the mandibular cortex in Göttingen minipigs and in man. *J Craniomaxillofac Surg*. 2002;30:219–225.
42. Cuccia AM, Caradonna C, Caradonna D, et al. The arterial blood supply of the temporomandibular joint: An anatomical study and clinical implications. *Imaging Sci Dent*. 2013;43:37–44.
43. Wysocki J, Reymond J, Krasucki K. Vascularization of the mandibular condylar head with respect to intracapsular fractures of mandible. *J Craniomaxillofac Surg*. 2012;40:112–115.
44. Mérida Velasco JR, Rodríguez Vázquez JF, Jiménez Collado J. Anterior tympanic artery: Course, ramification and relationship with the temporomandibular joint. *Acta Anat (Basel)* 1997;158:222–226.
45. Gharb BB, Rampazzo A, Kutz JE, Bright L, Doumit G, Harter TB. Vascularization of the facial bones by the facial artery: Implications for full face allotransplantation. *Plast Reconstr Surg*. 2014;133:1153–1165.
46. Fischer S, Lee TC, Krezdorn N, et al. First lower two-thirds osteomyocutaneous facial allograft perfused by a unilateral facial artery: Outcomes and vascularization at 1 year after transplantation. *Plast Reconstr Surg*. 2017;139:1175e–1183e.
47. Molnar G, Plachtovics M, Baksa G, Patonay L, Mommaerts MY. Intraosseous territory of the facial artery in the maxilla and anterior mandible: Implications for allotransplantation. *J Craniomaxillofac Surg*. 2012;40:180–184.
48. Dorafshar AH, Bojovic B, Christy MR, et al. Total face, double jaw, and tongue transplantation: An evolutionary concept. *Plast Reconstr Surg*. 2013;131:241–251.
49. Böckmann R, Meyns J, Dik E, Kessler P. The modifications of the sagittal ramus split osteotomy: A literature review. *Plast Reconstr Surg Glob Open* 2014;2:e271.